Magnetic transitions in $La_{1-x}Y_xMn_2Si_2$ - Mössbauer investigation (4.2-520 K)

1999 J. Phys.: Condens. Matter 11 7835

(http://iopscience.iop.org/0953-8984/11/40/310)

J. Phys.: Condens. Matter **11** (1999) 7835–7850. Printed in the UK PII: S0953-8984(99)04027-8

Magnetic transitions in $La_{1-x}Y_xMn_2Si_2$—Mössbauer investigation (4.2–520 K)

S J Campbell†‖, J M Cadogan‡, X L Zhao†, M Hofmann§ and Hong-Shuo Li‡

† School of Physics, University College, The University of New South Wales, Australian Defence Force Academy, Canberra, ACT 2600, Australia
‡ School of Physics, The University of New South Wales, Sydney, NSW 2052, Australia
§ Hahn–Meitner-Institut, BENSC, Glienickerstrasse 100, 14109 Berlin, Germany

E-mail: stewart.campbell@adfa.edu.au

Received 6 May 1999

Abstract. A set of eight tetragonal $La_{1-x}Y_xMn_2Si_2$ compounds doped with ^{57}Fe and covering the entire range $0 \leqslant x \leqslant 1$ have been investigated by Mössbauer effect spectroscopy over the temperature range 4.2–520 K. Distinct changes in the quadrupole splitting (QS) and magnetic hyperfine field ($\mu_0 H_{hf}$) values were observed around critical concentrations of $x_c \sim 0.15$ (4.2 K) and $x_c \sim 0.2$ (room temperature; RT) as the antiferromagnetism of the Y-rich compounds gives way to the predominant ferromagnetism of the La-rich compounds. The temperature dependences of QS and $\mu_0 H_{hf}$ for the La-rich compounds ($x \leqslant 0.25$) also show distinct changes in the range ∼285–470 K which we relate to the reported magnetic phase transitions occurring in these critical regions. The magnetic phase diagram which we have derived for the $La_{1-x}Y_xMn_2Si_2$ series from our Mössbauer measurements is in excellent agreement with the recent findings of neutron diffraction investigations. We show that analyses of both the Mössbauer and neutron data on $LaMn_2Si_2$ give a fully consistent account of the temperature dependent canting of the magnetic structure. Finally, consistent with earlier magnetization measurements, we suggest that a magnetically frustrated state, possibly a spin glass, may exist within the boundary regions of these magnetic phase transitions.

1. Introduction

The ternary rare-earth (R) manganese silicides RMn_2Si_2 crystallize in the tetragonal $ThCr_2Si_2$ structure with space group $I4/mmm$ [1]. This structure can be described as a stacking of atomic layers (each layer containing one single type of atom) along the crystallographic c-axis with the sequence –R–Si–Mn–Si–R. In the ideal $ThCr_2Si_2$ structure, each type of atom occupies one single crystallographic site; the site occupancies of the R(Th), Mn(Cr) and Si are 2a (0, 0, 0), 4d (0, 0.5, 0.25 and 0.5, 0, 0.25) and 4e (0, 0, z and 0, 0, $\bar{z}$) respectively. The structure can also be described as composed of silicon tetrahedra and rare-earth tetrahedra with manganese atoms inside. To form ideal tetrahedra the position parameter z and the ratio of lattice parameters (c/a) should be 3/8 and 2.818 respectively, with any deviation from these ideal values producing a distortion of the tetrahedra.

The magnetic properties of RMn_2X_2 (X = Si, Ge) have been studied extensively in the past two decades or so (see e.g. [2], [3] and references therein), with earlier reports describing relatively simple pictures for the magnetic structure of the RMn_2Si_2 compounds.

‖ Corresponding author.

0953-8984/99/407835+16$30.00

Magnetic susceptibility studies indicated that all of the compounds are antiferromagnetic except for R = La where ferromagnetic ordering is observed [2]. Neutron diffraction studies (e.g. [4]) revealed that the Mn magnetic moments couple ferromagnetically within the Mn layers and antiferromagnetically between adjacent Mn layers. Moreover, on the basis of single-crystal magnetization measurements on the isostructural $LaMn_2Ge_2$ compound, it was deduced that the magnetically easy direction of the Mn moments is along the c-axis [5]. A ferromagnetic to antiferromagnetic transition has been reported by magnetic susceptibility and neutron diffraction experiments in the systems $La_{1-x}Ce_xMn_2Si_2$ [6], $La_{1-x}Y_xMn_2Si_2$ [7, 8] and $La_{1-x}Y_xMn_2Ge_2$ [9], with the critical concentrations for these systems at room temperature being around $x_c \sim 0.4$, ∼0.2 and ∼0.7, respectively. A magnetic-field-induced AF to F transition has also been observed for $La_{0.3}Y_{0.7}Mn_2Ge_2$ below 170 K [10]. As shown in our recent Mössbauer effect measurements of the $La_{1-x}Y_xMn_2Si_2(^{57}Fe)$ series, distinct changes are observed in the hyperfine interaction parameters for samples around the critical concentrations $x_c \sim 0.15$ and $x_c \sim 0.20$ at 4.2 K [11] and room temperature [12], respectively.

YMn_2Si_2 has a magnetic structure of ferromagnetic Mn layers coupled antiferromagnetically with neighbouring layers, with a Néel temperature $T_N \sim 510$ K [3, 4, 8, 13] and magnetic space group $I_p4/m'm'm'$. Recent neutron diffraction [14, 15] and Mössbauer effect measurements [16–17] reveal a more complicated magnetic behaviour for $LaMn_2Si_2$ than considered previously (see e.g. [2], [3]). Nowik and co-workers (see e.g. [16]–[20]) have carried out detailed studies of the temperature dependences of the magnetic hyperfine interaction and the effective quadrupole interaction for a series of RMn_2Si_2 and RMn_2Ge_2 compounds (R = La, Ce, Pr, Nd, Sm and Gd), leading to insight into new multiple magnetic transitions in these and related materials. Below the Néel temperature $T_N \sim 470$ K, $LaMn_2Si_2$ exhibits collinear antiferromagnetism characterized by a stacking of antiferromagnetic (001) Mn planes (space group $Imm'm$) [14, 15]. Below $T_C \sim 310$ K, $LaMn_2Si_2$ exhibits an easy-axis ferromagnetic behaviour with the coexistence of an antiferromagnetic component in the (001) Mn planes in an overall canted magnetic structure (space group $I11m$). In addition, satellites to the (101) reflection are observed which are consistent with a conical magnetic arrangement coexisting with the canted magnetic structure below $T_h \sim 45$ K [14, 15].

Interest in the magnetic behaviour of RMn_2X_2 compounds has continued unabated in recent years with the comprehensive neutron diffraction investigations of Venturini and co-workers leading to novel insight into the magnetic structures and behaviour of compounds such as $Nd_{0.35}La_{0.65}Mn_2Si_2$ [21] and RMn_2Ge_2 [22]. More recently Hofmann *et al* [23] have determined the three magnetic structures exhibited by $La_{1-x}Y_xMn_2Si_2$ at the critical concentration $x_c \sim 0.2$ over the temperature range 4.2–500 K, with the magnetic phase diagram for this series having been determined by Ijjaali *et al* [24]. Here we extend our earlier Mössbauer effect studies of $La_{1-x}Y_xMn_2Si_2(^{57}Fe)$ at 4.2 K and ambient temperature to investigate the magnetic behaviour of the set of eight samples over the temperature range 4.2–520 K. The temperature dependences of the quadrupole splitting and magnetic hyperfine field values have enabled the magnetic transitions and overall magnetic behaviour to be determined. The resultant magnetic phase diagram is found to be in good agreement with the results of our concurrent neutron diffraction studies of $La_{1-x}Y_xMn_2Si_2$ on the same set of samples [15, 25, 26].

2. Experiment

The $La_{1-x}Y_xMn_2Si_2(^{57}Fe)$ ($x = 0.00$, 0.10, 0.15, 0.20, 0.25, 0.30, 0.50 and 1.00) samples were prepared by conventional argon arc melting from elements of >3 N purity. The samples were doped with enriched ^{57}Fe of amounts ∼0.3–0.5 wt%. X-ray powder diffraction indicated

that all the samples were single phase with the tetragonal $ThCr_2Si_2$ structure. Standard ^{57}Fe Mössbauer effect spectroscopy measurements were carried out in transmission mode over the temperature range 4.2–520 K. Low temperature experiments (4.2–300 K) were performed using a helium-bath cryostat and a LakeShore DRC-93C temperature controller, while high temperature experiments (300–520 K) were carried out using a temperature-controlled vacuum furnace. The spectrometer was calibrated using a standard α-Fe foil.

3. Results and discussion

Mössbauer spectra were obtained for the complete set of $La_{1-x}Y_xMn_2Si_2$(^{57}Fe) samples at various temperatures between 4.2 K and 520 K. Typical results for the $La_{0.85}Y_{0.15}Mn_2Si_2$ sample are shown in figure 1.

The model which we used to fit the spectra over this series has been described previously [11, 12]. In brief, based on the results by Levin *et al* [27] on the $CeM_{2-x}Si_{2+x}$ series (M = Fe, Co, Ni and Cu), it is expected that the ^{57}Fe atoms will enter the Mn crystallographic 4d site predominantly. Given the equal number of Mn and Si in the $La_{1-x}Y_xMn_2Si_2$ compounds, it is clear that even if only ∼0.1% of the Si atoms are replaced by the ^{57}Fe atoms, then ∼10% of the ^{57}Fe atoms would reside on the Si 4e site. Comparison of fits to the spectra with one sextet (representing sole occupancy of the 4d site by ^{57}Fe atoms) or two sextets (^{57}Fe atoms in both the 4d and 4e sites) confirms that the best fits of the spectra were obtained using two sextets, consistent with the likelihood that ^{57}Fe atoms enter both the Mn 4d (sextet I) and Si 4e sites (sextet II) [11]. Given the poor resolution of the spectra taken close to or above the ordering temperatures, the fits were carried out by restricting the intensity ratios of the two subspectra to the values obtained at low temperatures. Sextet I with a larger subspectral area, A^I, and a larger magnetic hyperfine field than sextet II is associated with the ^{57}Fe atoms in the Mn 4d site, with sextet II being associated with the ^{57}Fe atoms in the Si 4e site (see also [17]). As indicated in table 1, the ^{57}Fe atoms show a non-negligible occupation of the Si 4e site in all of the $La_{1-x}Y_xMn_2Si_2$ samples studied although, as expected, there is a marked preference of ^{57}Fe atoms to occupy the Mn 4d site, with the relative subspectral area for the 4d site varying from 87 to 94% over our set of samples. These site occupancies lead to slight distributions in the hyperfine parameters, as manifested by the line broadening.

Table 1. Subspectral intensities (A^I) and ratios of magnetic hyperfine fields ($\mu_0 H^I_{hf}/\mu_0 H^{II}_{hf}$) derived from fits to the 4.2 K $La_{1-x}Y_xMn_2Si_2$(^{57}Fe) spectra (see also [11]).

	$x = 0.00$	$x = 0.10$	$x = 0.15$	$x = 0.20$	$x = 0.25$	$x = 0.30$	$x = 0.50$	$x = 1.00$
A^I (%)	92(3)	87	90	89	92	88	94	88
$\mu_0 H^I_{hf}/\mu_0 H^{II}_{hf}$	2.3(5)	3.0	2.4	2.9	2.6	3.1	2.9	3.3

As shown in table 1, the magnetic hyperfine fields for the two subspectra I and II are found to differ by a factor of ∼3. As discussed previously [11], this ratio agrees well with the ratio of the hyperfine fields calculated on the basis of the direct anisotropic exchange interaction from the nearest-neighbour Mn atoms. Due to the small intensity of subspectrum II, the corresponding hyperfine parameters deduced from the spectral fits contain relatively large uncertainties although the presence of subspectrum II causes no significant change in the fitted hyperfine parameters of the dominant subspectrum I. In our discussion, we concentrate on the significance of the hyperfine parameters obtained for subspectrum I, i.e. the subspectrum of ^{57}Fe atoms in the Mn 4d site.

3.1. Dependence of the hyperfine parameters on yttrium concentration

The dependence of the ^{57}Fe hyperfine field $\mu_0 H_{hf}^I$ on the yttrium concentration is shown in figure 2. At 4.2 K the value of $\mu_0 H_{hf}^I$ is essentially constant in the concentration range $x = 0.0$–0.15, whereas above $x \sim 0.15$, the value of $\mu_0 H_{hf}^I$ increases linearly with a slope of $\mathrm{d}(\mu_0 H_{hf}^I)/\mathrm{d}x = 3.4$ T at.%$^{-1}$. The change in the behaviour of $\mu_0 H_{hf}^I$ around $x = 0.15$ reflects a magnetic phase transition, indicating that the magnetic structure of $La_{1-x}Y_xMn_2Si_2$ compounds in this region is highly sensitive to the yttrium concentration. With increasing temperature, a minimum in the magnetic hyperfine field becomes apparent at the critical concentration of $x \sim 0.2$. As expected, the behaviour of the magnetic hyperfine field essentially reflects the variation in transition temperatures T_C and T_N which also exhibits a minimum value around the yttrium concentration of $x \sim 0.2$ (see figure 7 as discussed below).

The dependence of the ^{57}Fe quadrupole splitting (QS) on the yttrium concentration at different temperatures is shown in figure 3. A step-like dependence around $x \sim 0.2$ is observed at all temperatures except for $T \sim 450$–520 K, where all the compounds are in the paramagnetic state. A distinct change occurs in the QS between the two magnetic phases—the antiferromagnetism with ferromagnetic Mn layers for $x > \sim 0.2$ and the canted magnetic structures for $x < \sim 0.2$ when $T < \sim 305$ K (or antiferromagnetism with antiferromagnetic Mn layers when $T > \sim 305$ K). The change in the QS between the F and AF regions is a consequence of the change in the 3d configuration of the probe ^{57}Fe atoms which reflects the corresponding change of the Mn 3d configuration. The quadrupole interaction can be described in terms of the electric field gradient (EFG) tensor $\{V_{ij}\}$. In the $ThCr_2Si_2$ type structure the Mn(Cr) atoms occupy the 4d site which has a local point symmetry of $\bar{4}m2$. In this case, we can then explicitly write the total V_{ZZ} as [28]:

$$V_{ZZ} = (1 - \gamma_\infty)V_{ZZ}^{latt} + (1 - R)V_{ZZ}^{val} \tag{1}$$

where γ_∞ and R are the Sternheimer antishielding and shielding factors, respectively. The two terms in equation (1) represent: (i) the lattice contribution V_{ZZ}^{latt} which arises from the non-cubic symmetry of the surrounding charges on neighbouring atoms and (ii) the valence contribution V_{ZZ}^{val} which results from the electron distribution in the partially filled valence shell of the ^{57}Fe atom (3d and 4p shells). The c-axis is the easy magnetization direction of the Mn sublattice for YMn_2Si_2 (see e.g. [4], [13]). On the other hand, recent studies have shown that $LaMn_2Si_2$ has a canted magnetic structure below $T_C \sim 310$ K with a canting angle of $\sim 47^\circ$ relative to the c-axis at low temperatures [14, 15].

Our point charge model calculations show that V_{ZZ} is along the c-axis in the RMn_2Si_2 structure, while the asymmetry parameter is $\eta = 0$, indicating an axially symmetric EFG. As discussed more fully below, a change of the hyperfine field direction from a canting angle of 47° to 90° results in a change in the magnitude and sign of the QS as is observed in the experimental data. Furthermore, at room temperature, for $La_{1-x}Y_xMn_2Si_2$ compounds with $x \sim 0.2$ (canted antiferromagnetic structure as discussed below [24, 25]), the QS value is significantly different from those compounds with $x > 0.3$ ($I_p4/m'm'm'$; collinear ferromagnetic layers coupled antiferromagnetically). This suggests that although V_{ZZ}^{latt} may vary between the two magnetically ordered states, the major contribution to the change in QS between these two states is due to valence effects. Hence, the change in the quadrupole splitting observed between the ferromagnetic and antiferromagnetic regions in the $La_{1-x}Y_xMn_2Si_2$ series is most likely to be the result of differences in the 3d configurations between these two magnetically ordered states. We note that the Mn–Si distance in these compounds is very short, ranging from 0.234 nm ($x = 1$) to 0.243 nm ($x = 0$). Based on metallic radius data [29] the expected Mn–Si distance is 0.258 nm ($r_{Mn} = 0.127$ nm and $r_{Si} = 0.131$ nm), which would correspond to no overlapping of

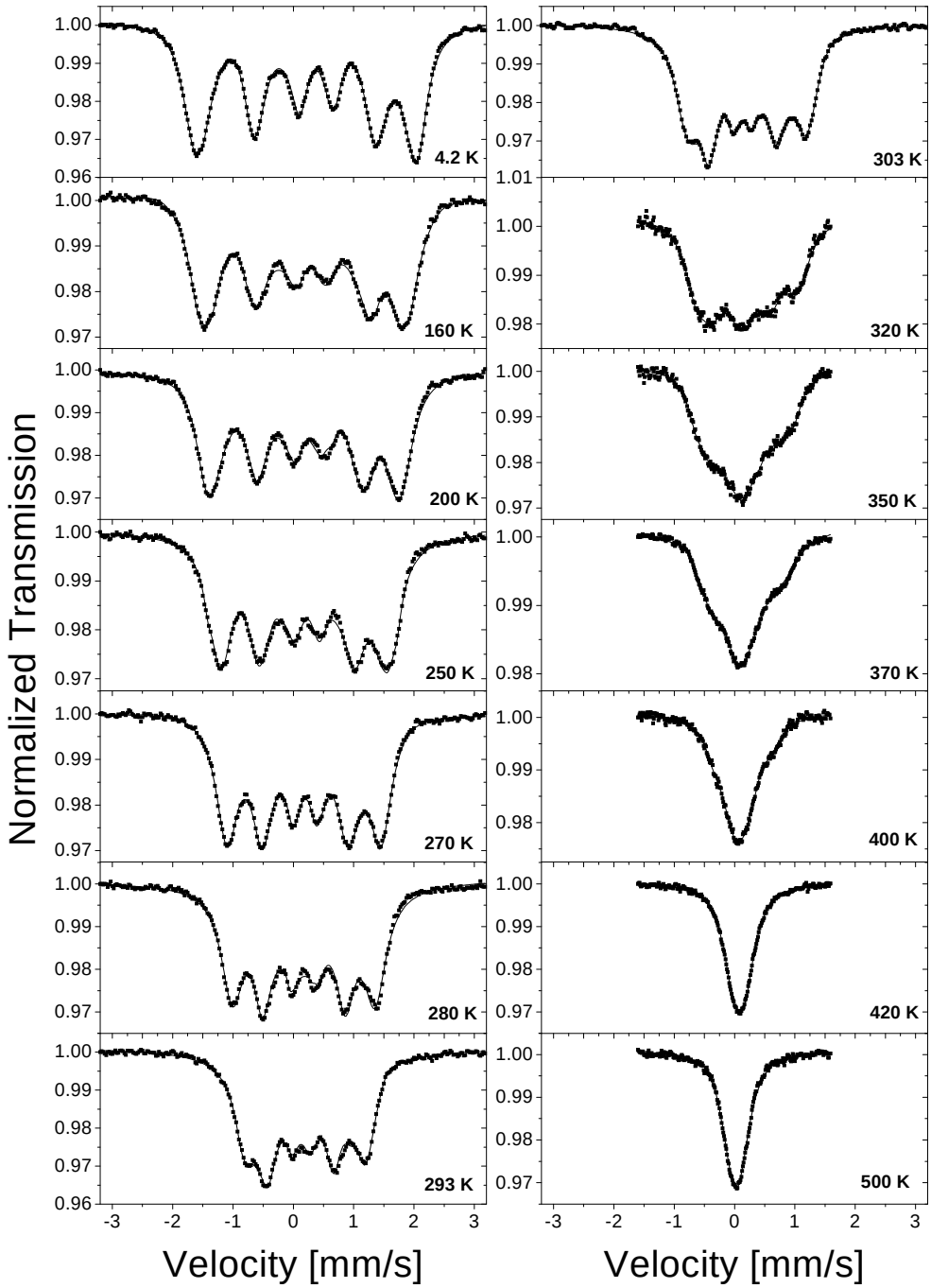

Figure 1. Mössbauer spectra of ^{57}Fe doped $La_{0.85}Y_{0.15}Mn_2Si_2$ at the temperatures indicated. All of the spectra have been fitted with two subspectra as described in the text.

the valence bands. Thus, we attribute the major contribution to the changes in the QS between the ferromagnetic and antiferromagnetic states to a change in the 3d electronic configuration

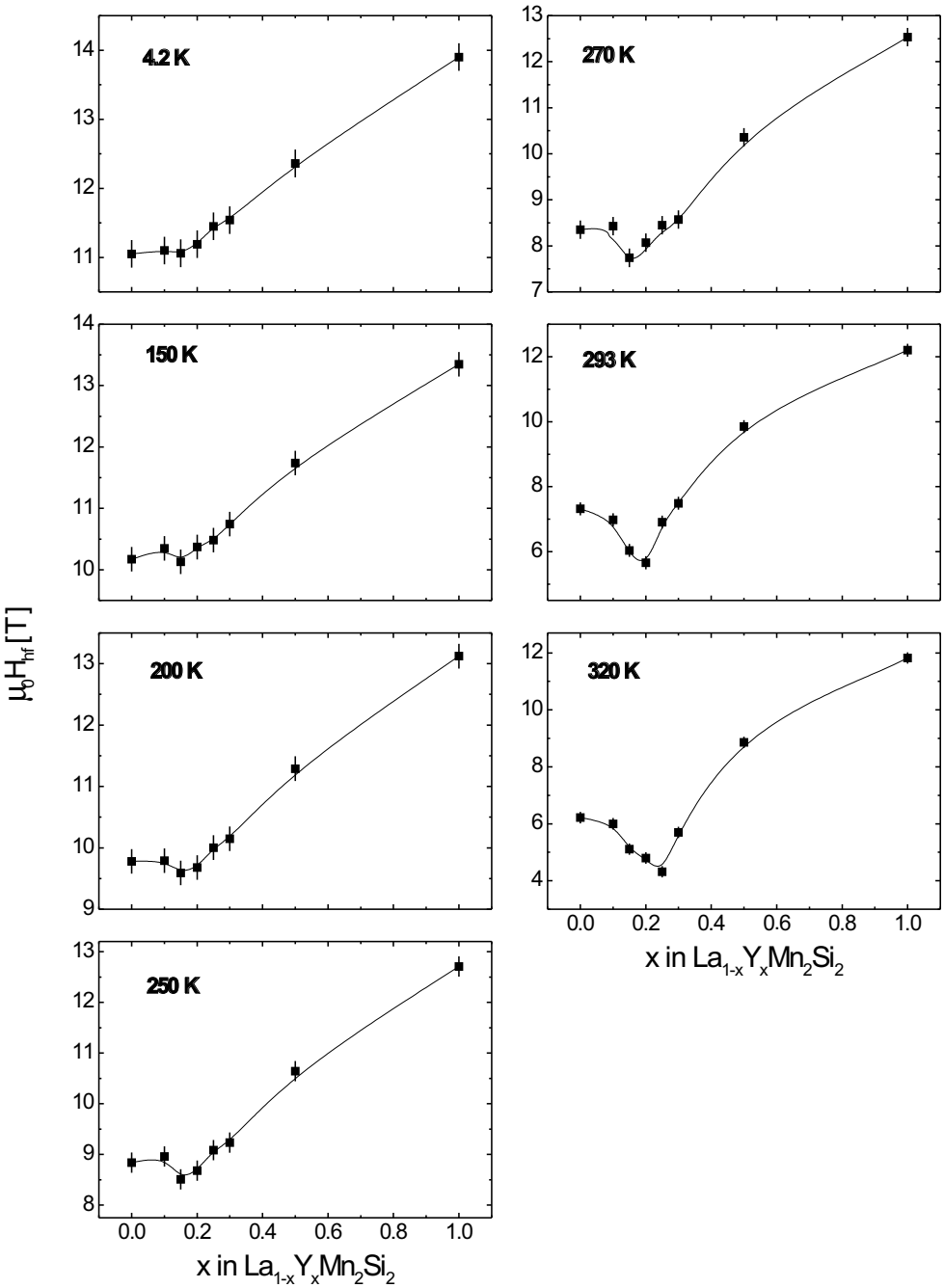

Figure 2. Variation of the magnetic hyperfine field of $La_{1-x}Y_xMn_2Si_2$ (^{57}Fe) with Y concentration at the temperatures indicated (4.2–320 K) (the full lines act as a guide to the eye).

caused by increased hybridization between the Mn 3d band and Si 3p band; a reduction in the unit cell volume and interatomic distances leads to a greater charge transfer from the Si to the Mn (^{57}Fe) atoms. Recent LMTO energy band calculations on the paramagnetic states of

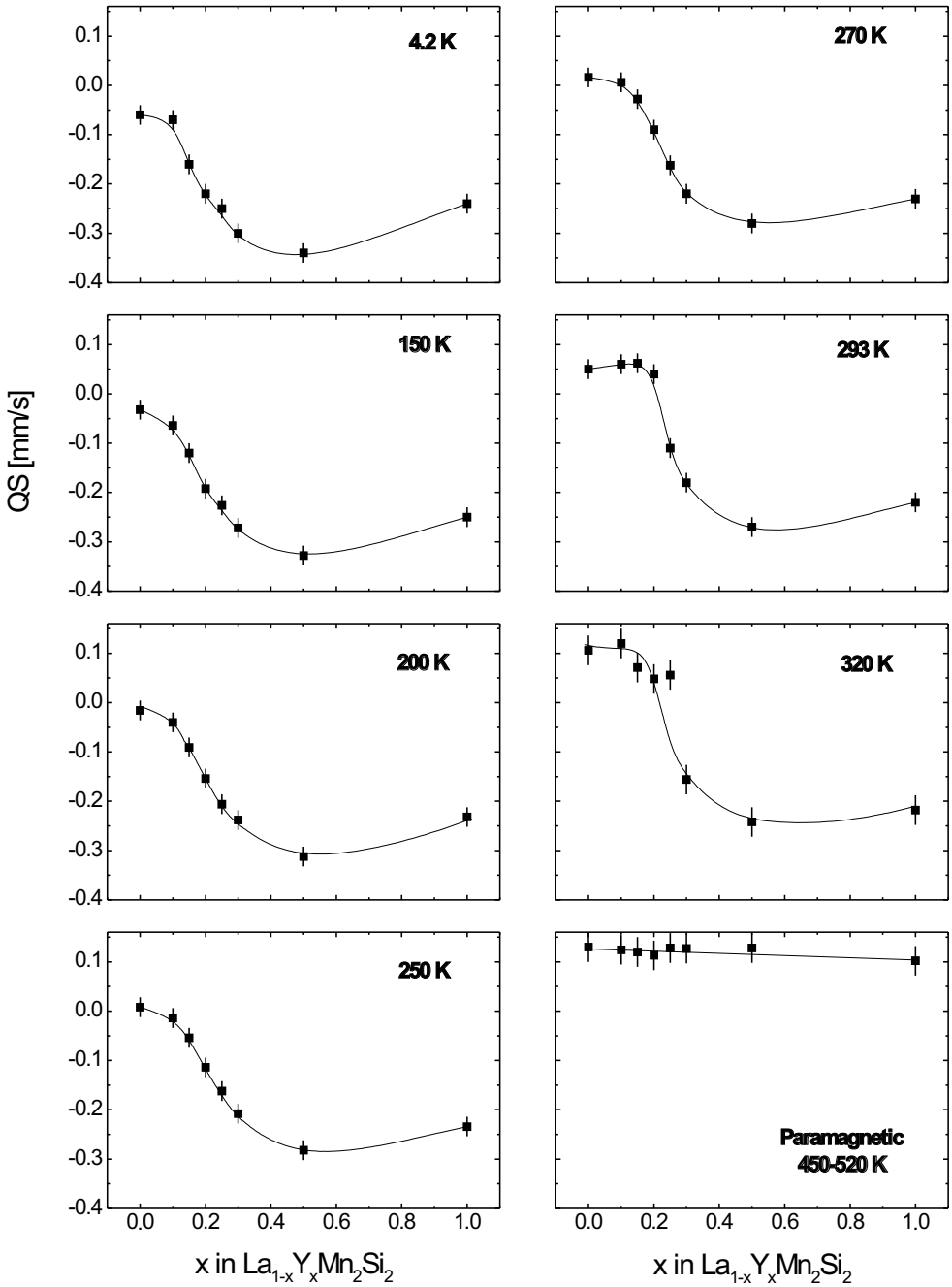

Figure 3. Variation of the quadrupole splitting of $La_{1-x}Y_xMn_2Si_2$ (^{57}Fe) with Y concentration at the temperatures indicated (4.2–520 K) (the full lines act as a guide to the eye).

$LaMn_2Si_2$ and YMn_2Si_2 [30, 31] show that there is in fact a strong hybridization between the Mn 3d band and Si 3p band, and the electron transfer from Si to Mn is greater in YMn_2Si_2 than in $LaMn_2Si_2$. The valence component, V_{ZZ}^{val} is tightly linked to the relative occupancies of the

3d states (denoted t_{2g} or e_g); any change in these occupancies will cause a change in V_{ZZ}^{val}. Hence, the change in the quadrupole splitting observed can mainly be explained by differences in the 3d configurations between these two magnetically ordered states.

In summary, it is clear that the two principal hyperfine parameters, i.e. magnetic hyperfine field and quadrupole splitting at various temperatures provide useful information on the changes in the Mn electronic structure associated with the magnetic phase transitions in the $La_{1-x}Y_xMn_2Si_2$ series. As discussed fully below, at 4.2 K $La_{1-x}Y_xMn_2Si_2$ compounds with $x < \sim 0.10$ have a canted ferromagnetic structure whereas those compounds with $x > \sim 0.10$ exhibit antiferromagnetic behaviour (see e.g. [23]–[25]); see also figure 7). Likewise at room temperature, the $La_{1-x}Y_xMn_2Si_2$ series for $x < \sim 0.15$ exhibits canted ferromagnetism which changes to antiferromagnetism for higher Y concentrations ($x > \sim 0.15$).

3.2. Temperature dependence of the hyperfine parameters

The temperature dependences of the magnetic hyperfine field and the quadrupole splitting of sextet I as determined from the fits to the $La_{1-x}Y_xMn_2Si_2(^{57}Fe)$ spectra, are presented in figures 4 and 5, respectively. $La_{0.85}Y_{0.15}Mn_2Si_2$ with a concentration close to the critical concentration of $x_c = 0.2$ at RT exhibits a magnetic transition around $T_C = 290$ K (figure 4, also see [8]). The Mössbauer spectra and $\mu_0 H_{hf}$ data of the present sample show clearly that the magnetic hyperfine field persists above the apparent magnetic ordering temperature of $T = 290$ K, suggesting that the Mn sublattice remains ordered above this temperature. Similar behaviour is observed for all La-rich $La_{1-x}Y_xMn_2Si_2(^{57}Fe)$ compounds ($x \leqslant 0.25$, figure 4) and as noted above, similar behaviour was observed recently for $LaMn_2Si_2(^{57}Fe)$ [16, 17]. At temperatures above ∼310 K, $LaMn_2Si_2$ exhibits collinear antiferromagnetism [14, 15]. Our findings indicate that the antiferromagnetic order in these La-rich compounds exists within the Y concentration region $0 < x < 0.3$, and within the temperature region 285–470 K.

Clear insight into the high temperature magnetic behaviour of $La_{0.85}Y_{0.15}Mn_2Si_2(^{57}Fe)$ can be derived from the hyperfine parameters. The kink in the $\mu_0 H_{hf}$ values for sextet I at $T = 290$ K (see arrow, figure 4), combined with the distinct changes in QS at the same temperature (figure 5), identify a magnetic transition from the low temperature canted magnetic structure. Although the sample $La_{0.85}Y_{0.15}Mn_2Si_2$ lies in the critical concentration region between the canted ferromagnetism of $LaMn_2Si_2$ and the antiferromagnetism of YMn_2Si_2, the present transition at $T = 290$ K describes a temperature driven magnetic phase transition, probably similar to that observed by Venturini *et al* [14] in $LaMn_2Si_2$. The magnetic hyperfine field for sextet I continues to decrease above T_C, leading to a Néel temperature $T_N \sim 425$ K (figure 4). The hyperfine parameters of $La_{1-x}Y_xMn_2Si_2$ compounds with $x < 0.3$ may be analysed in a similar manner, leading to their T_C and T_N values. On the other hand, compounds with $x > 0.3$ show no evidence of a change in the magnetic structure below their Néel temperature. As noted above, the QS values for the dominant sextet I of $La_{0.85}Y_{0.15}Mn_2Si_2(^{57}Fe)$ change significantly around the transition at $T_C = 290$ K (figure 5). As discussed above a lattice contribution to the observed changes in QS values may be present, although the change in the observed quadrupole splitting is most likely to be due to a change in QS^{val} with differences in the 3d configurations between the two magnetically ordered states.

As discussed by Venturini *et al* [21] the unusual variation with temperature of the electric quadrupole parameter as determined by Mössbauer spectroscopy, can be accounted for in terms of the relative orientation (angle θ) of V_{ZZ}, the principal component of the electric field gradient (EFG) tensor, and the Mn magnetic moment (and hence the hyperfine magnetic field experienced by the ^{57}Fe nuclei). As mentioned above, the principal z-axis coincides with the crystallographic c-axis and the point symmetry $\bar{4}m2$ of the Mn site axial symmetry (i.e. the

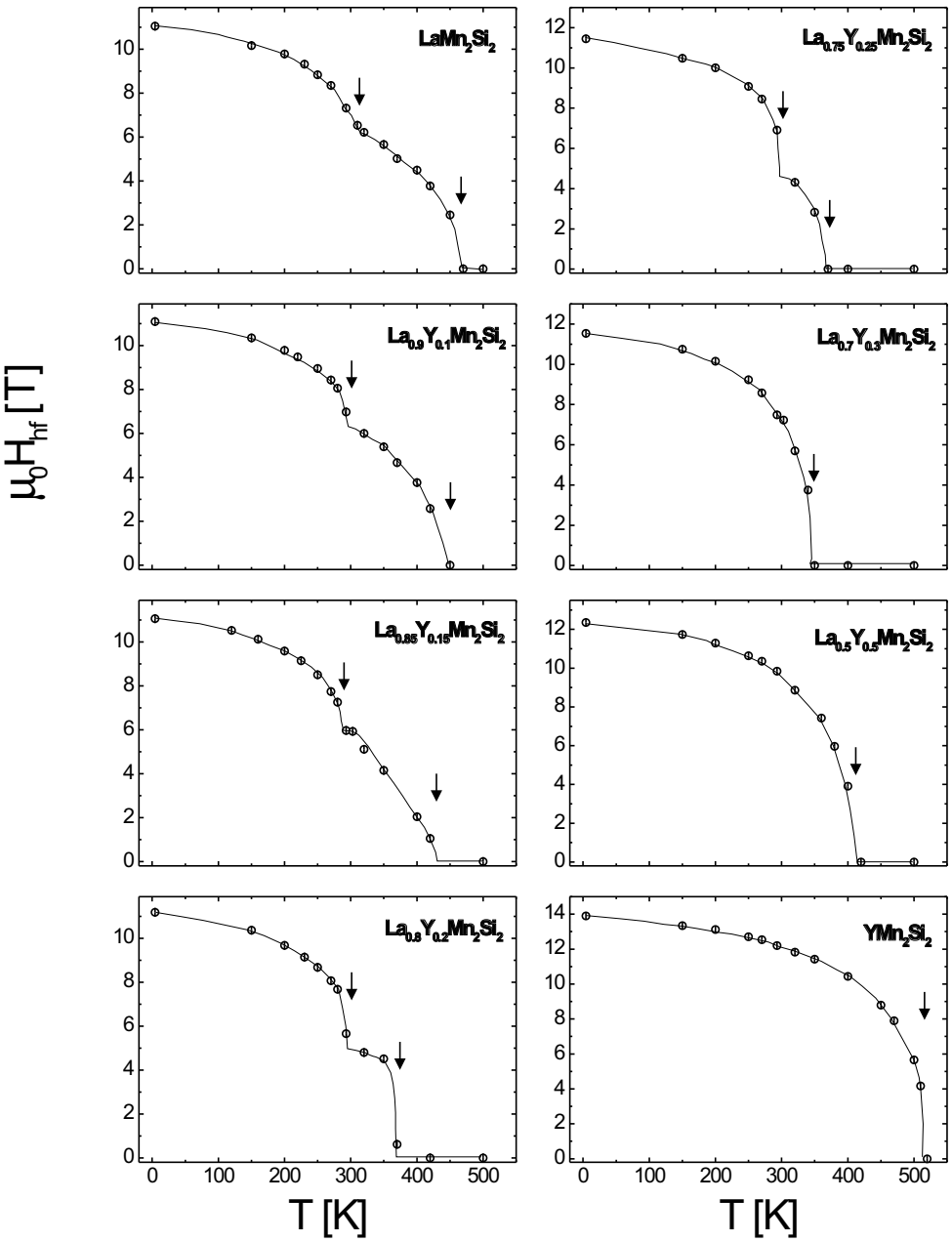

Figure 4. Temperature dependence of the magnetic hyperfine field for $La_{1-x}Y_xMn_2Si_2$(^{57}Fe). The arrows indicate the magnetic transition temperatures (the full lines act as a guide to the eye).

asymmetry parameter $\eta = 0$). The relevant angular dependent term in the nuclear Hamiltonian is then: $(3\cos^2\theta - 1)/2$. Given the orientation of the EFG principal axis system, the angle θ can be measured directly by neutron diffraction, which gives the angle between the magnetic moment and the crystal c-axis.

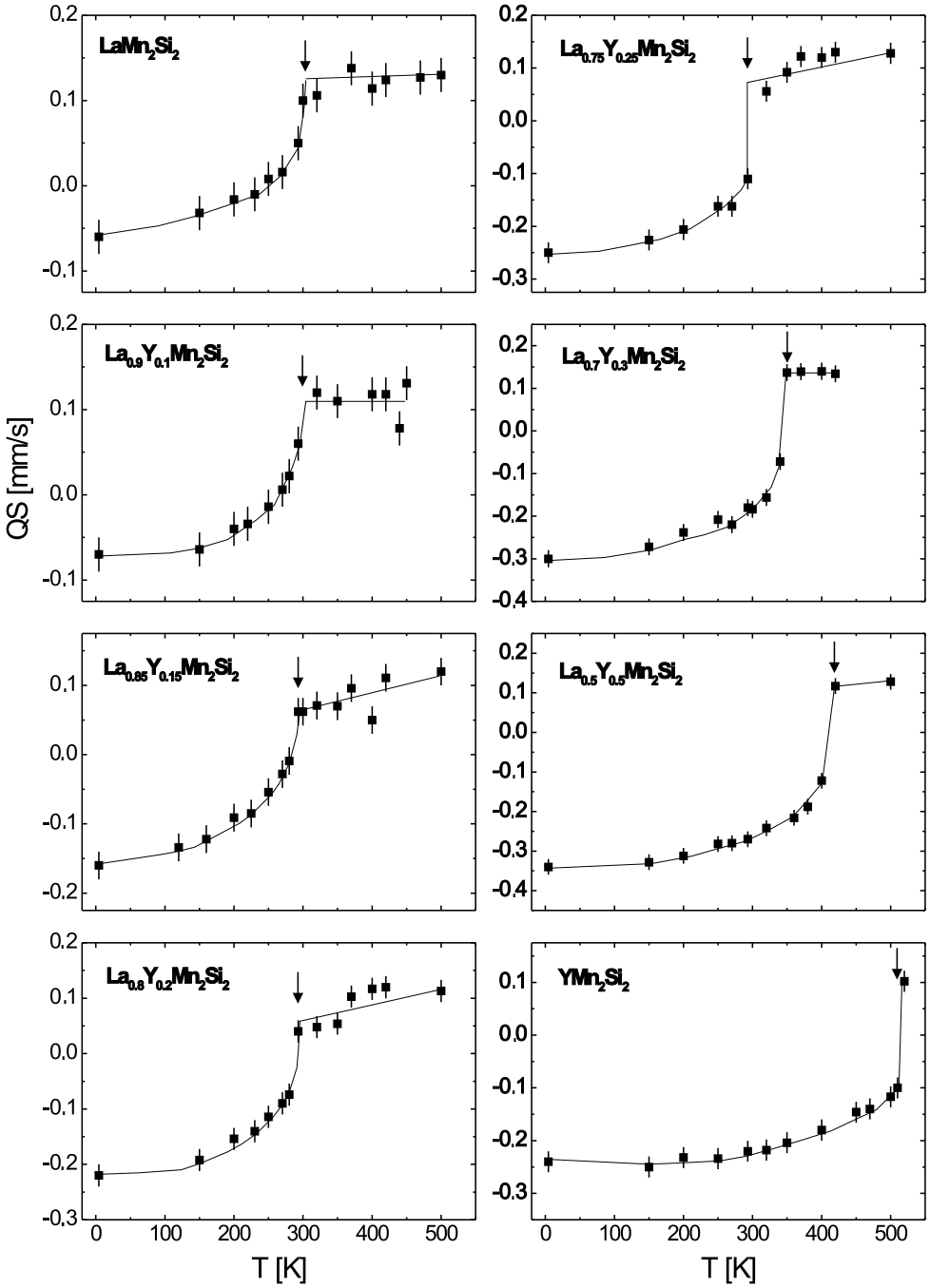

Figure 5. Temperature dependence of the quadrupole splitting for $La_{1-x}Y_xMn_2Si_2$ (^{57}Fe). The arrows indicate the magnetic phase transition temperatures (the full lines act as a guide to the eye).

In figure 6 we show the orientation of the Mn magnetic moments (i.e. θ) in $LaMn_2Si_2$ deduced both from our Mössbauer results and from our concurrent neutron diffraction work

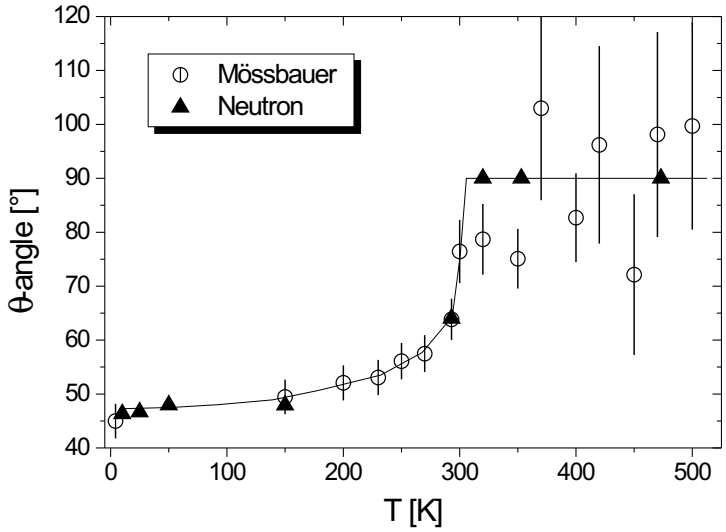

Figure 6. Temperature dependence of the canting angle (θ) relative to the c-axis, of the Mn moments in $LaMn_2Si_2$ as deduced from our Mössbauer and neutron diffraction measurements (the full line acts as a guide to the eye).

on this compound. The neutron results show clearly that the magnetic moments lie in the crystallographic basal plane between $T_C \sim 310$ K and $T_N \sim 470$ K. We therefore took the average value of the quadrupole splitting in this temperature range as our starting value for the determination of θ from the Mössbauer data. The collapse in the hyperfine splitting with increase in temperature makes it difficult to determine the quadrupole parameter with a high degree of accuracy in the temperature range between the two magnetic ordering temperatures. This limited spectral resolution leads to the scatter in the deduced θ values between ∼350 and 450 K (figure 6). Also it should be noted that this analysis is strictly valid only when the magnetic hyperfine splitting is much greater than the electric quadrupole interaction. This results in increased uncertainty in the θ values at higher temperatures as the magnetic hyperfine field collapses. Below the Curie temperature (∼310 K) there is excellent agreement between the two determinations of θ showing the gradual tipping of the moments out of the crystallographic basal plane with decreasing temperature, thus establishing that for $LaMn_2Si_2$ the observed variation in quadrupole splitting is due to the changing magnetic moment orientations.

3.3. Phase transitions

The magnetic phase diagram deduced for the $La_{1-x}Y_xMn_2Si_2$ series from our Mössbauer data is shown in figure 7 with the transition temperatures, as derived from the discontinuities in QS (T_C) and the collapse of the hyperfine field (T_N), listed in table 2. The T_C values for $x < 0.3$ and the T_N values for $x > 0.3$ are in agreement with previous studies [8, 24]. The magnetic structures of this series of compounds (denoted in figure 7 using the notation of Venturini *et al* [21]) are as follows [14, 15, 24, 25]. La-rich compounds exhibit canted ferromagnetism (Fmc) and planar antiferromagnetism (AFl) with Y-rich compounds exhibiting axial antiferromagnetism (AFil). Intermediate $La_{1-x}Y_xMn_2Si_2$ concentrations, around $x \sim 0.2$, also exhibit canted antiferromagnetism (AFmc; in effect a combination of AFl and AFil) and, as discussed recently [25], a region in which the two canted structures,

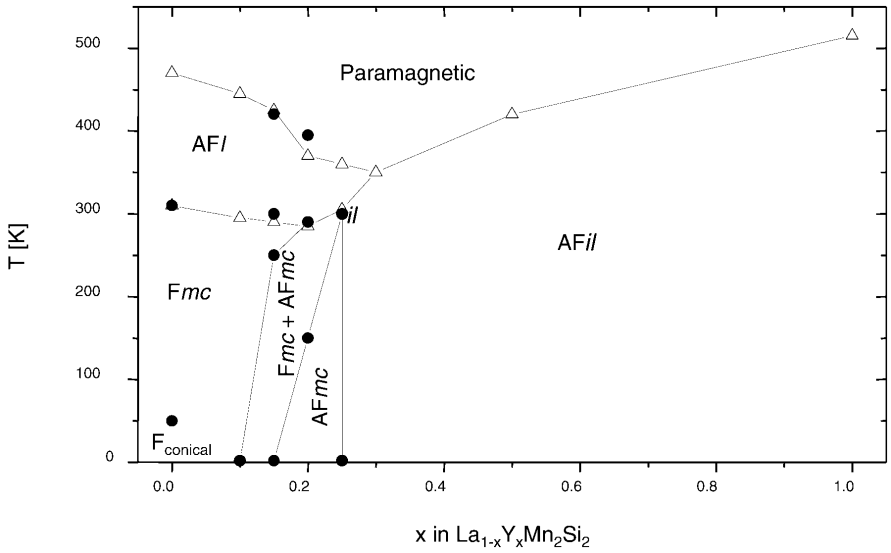

Figure 7. The magnetic phase diagram of $La_{1-x}Y_xMn_2Si_2$ as derived from our Mössbauer effect results and neutron diffraction data [15, 23, 25, 26]. The magnetic structures are labelled using the notation of Venturini *et al* [21] as follows: La-rich compounds—canted ferromagnetism (F*mc*) and planar antiferromagnetism (AF*il*); Y-rich compounds—axial antiferromagnetism (AF*il*); intermediate concentrations ($x \sim 0.2$)—canted antiferromagnetism (AF*mc*; in effect a combination of AF*l* and AF*il*) and, as discussed recently [25], a region in which the two canted structures, F*mc* and AF*mc*, coexist. $F_{conical}$ refers to the conical magnetic arrangement of $LaMn_2Si_2$ which co-exists with the canted magnetic structure below $T_h \sim 45$ K [14, 15].

Table 2. Transition temperatures T_C and T_N in $La_{1-x}Y_xMn_2Si_2$ compounds, as estimated (to $< \sim$10 K) from changes in the hyperfine parameters (figures 4 and 5).

	$x = 0.00$	$x = 0.10$	$x = 0.15$	$x = 0.20$	$x = 0.25$	$x = 0.30$	$x = 0.50$	$x = 1.00$
T_C (K)	310(10)	295	290	285	305	—	—	—
T_N (K)	470(10)	445	425	370	360	355	420	515

F*mc* and AF*mc*, coexist. The existence of these magnetic phase transitions suggests that the magnetic structure is very sensitive to the interatomic distances in these compounds. In the earlier literature all of the known magnetic structures of the $ThCr_2Si_2$-type manganese silicides and germanides were described in terms of ferromagnetic (001) Mn planes, stacked ferro-or antiferromagnetically along the *c*-axis [2]. Szytula and Siek [6] pointed out that intralayer Mn–Mn distances greater than ∼0.285 nm lead to ferromagnetic interplane interactions, whereas distances less than ∼0.285 nm lead to antiferromagnetic interplane interactions.

As noted above, recent investigations have resulted in a revised model of the magnetic structure of $LaMn_2Si_2$ [14, 15]. This compound was found to possess a canted structure at low temperatures and an antiferromagnetic structure above $T_C \sim 310$ K, with a conical magnetic arrangement (denoted $F_{conical}$ in figure 7) co-existing with the canted magnetic structure below $T_h \sim 45$ K [14, 15]. Under such circumstances a revision of the relationship between the intralayer Mn–Mn distance and the magnetic structure in the $La_{1-x}Y_xMn_2Si_2$ compounds is necessary. As pointed out by Venturini *et al* [14, 21], for the RMnSi(Ge) and $RMn_2Si(Ge)_2$ series, antiferromagnetic (001) Mn planes occur when the Mn–Mn intralayer separation is larger than ∼0.285 nm, whereas a smaller Mn–Mn intralayer distance yields ferri- or ferromagnetic Mn layers. From the experimental results for the $La_{1-x}Y_xMn_2Si_2$ compounds

(figure 7), it appears that while an Mn–Mn intralayer separation $d_{Mn-Mn} < 0.285$ nm is associated with a magnetic structure characterized by ferromagnetic Mn (001) planes coupled antiferromagnetically with their neighbouring planes, an Mn–Mn intralayer separation of $d_{Mn-Mn} > 0.285$ nm is linked with antiferromagnetic Mn(001) layers, or Mn(001) layers having a canted magnetic structure with antiferromagnetic components. This fulfils the general correlation between the Mn–Mn intralayer distance and the magnetic structure within the Mn layers, which has been confirmed in a large number of compounds with either the $ThCr_2Si_2$, CeFeSi or $TbFeSi_2$ structures [32]. The magnetic structure of $LaMn_2Si_2$ at low temperatures may be due to the fact that the antiferromagnetic (001) planes induce additional interplanar ferromagnetic interactions which begin to act when the thermal contraction of the lattice smooths out the antiferromagnetic in-plane interactions.

Williams *et al* [33] have suggested that the d–d exchange interaction mediated by p electrons causes antiferromagnetic ordering, based on the results of band calculations of Mn based Heusler alloys. This critical distance is close to the critical distance of 0.285 nm for the transition from localized to delocalized Mn states as predicted by Goodenough [34]. The substitution of Y for La leads to a decrease in the unit cell volume (and hence the interlayer and intralayer Mn–Mn distances) which in turn enhances the in-plane ferromagnetic interaction and weakens the in-plane antiferromagnetic interaction. At low yttrium concentrations ($x < 0.2$), where antiferromagnetic layers (or a canted structure) are present, these three types of interaction compete with each other, resulting in a decrease in the ordering temperature with increasing yttrium content. At larger yttrium concentrations ($x > 0.25$) the increase in the ordering temperature is considered to be due to the broadening of the Mn 3d band with increasing yttrium content.

3.4. Transition region: spin glass and frustrated magnetic system

The competition between the different interactions around the critical concentration $x_c \sim 0.2$ (RT) for the transition from one magnetic state to the other is believed to lead to spin glass [8] or cluster spin glass [7] type behaviour. The more complex magnetic behaviour occurring around this concentration is also indicated by the large difference in values between the magnetic transition temperature $T_C \sim 250$ K and the paramagnetic Curie temperature $\theta_p \sim 310$ K for a $La_{1-x}Y_xMn_2Si_2$ compound with $x = 0.2$, as estimated by Sampathkumaran *et al* [8] from magnetization and magnetic susceptibility measurements. Coexistence of different magnetic interactions and spin-glass-like behaviour is also likely to account for the increase in linewidth observed in the room temperature Mössbauer spectra of $La_{1-x}Y_xMn_2Si_2$ compounds for yttrium concentrations around $x \sim 0.15$–0.25 (figure 8). Further evidence for a spin-glass/frustrated system is the fact that the hyperfine magnetic field of subspectrum II (associated with the ^{57}Fe residing in the Si 4e site) does not vanish at T_C for compounds with $x < 0.3$, as shown in the case of the $La_{0.85}Y_{0.15}Mn_2Si_2$(^{57}Fe) compound (figure 9(a)). As outlined previously [35], with increasing temperature ^{57}Fe atoms in the Si 4e site within the antiferromagnetic (001) Mn layers continue to experience a transferred field until the balance between the exchange interactions of the antiparallel moments of the antiferromagnetic (001) Mn planes is established fully. For example the magnetic hyperfine field associated with sextet II in $La_{0.85}Y_{0.15}Mn_2Si_2$(^{57}Fe) persists from $T_C \sim 290$ K to a temperature $T_C^{II} \sim 340$ K. Hence, the gradual decrease in the $\mu_0 H_{hf}$ values for sextet II to zero over the temperature range $T = 290$–340 K (figure 9(a)) is likely to indicate the existence of a frustrated magnetic system in this region with competing interactions occurring both as a result of the temperature driven transition, and the critical dependence on the La and Y concentrations of the compound with $x < 0.3$. This behaviour is also found to occur for the $La_{1-x}Y_xMn_2Si_2$ compounds of

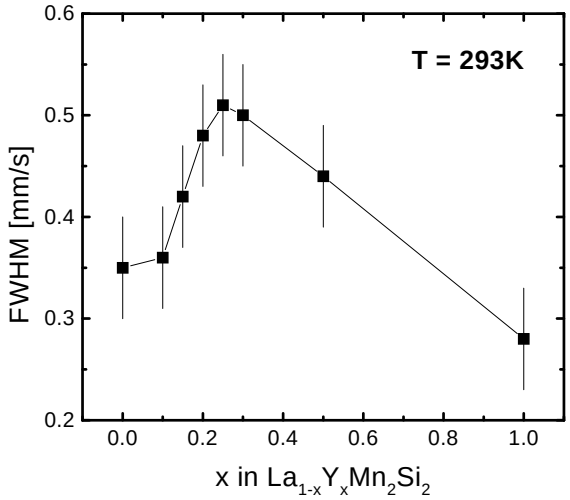

Figure 8. Dependence of the spectral linewidth (full width at half maximum) of the room temperature spectra of $La_{1-x}Y_xMn_2Si_2$ (^{57}Fe) on yttrium concentration.

Y concentration $x = 0.1$, 0.2, 0.25 with their T_C^{II} along with the T_C and T_N values, shown as a function of Y concentration in figure 9(b). As indicated by the above discussion, along the boundary of the different magnetic phases there exists a finite region in which spin-glass, clusters of spin-glass and/or frustrated magnetic systems are likely to occur.

4. Conclusions

The magnetic properties of $La_{1-x}Y_xMn_2Si_2$ compounds with $x = 0.00$, 0.10, 0.15, 0.20, 0.25, 0.30, 0.50 and 1.00 have been investigated by Mössbauer effect spectroscopy. The experimental results indicate that although most of the ^{57}Fe atoms occupy the Mn 4d site, there is a non-negligible fraction of the ^{57}Fe atoms residing in the Si 4e site. Distinct changes in QS and $\mu_0 H_{hf}$ are observed around the critical concentrations of $x_c \sim 0.15$ (4.2 K) and $x_c \sim 0.20$ (RT). The temperature dependences of the QS and $\mu_0 H_{hf}$ values in the spectra of the La-rich compounds $La_{1-x}Y_xMn_2Si_2$ (^{57}Fe) ($x \leqslant 0.25$) also show distinct changes in the range between ~285 and 470 K. These results are discussed in term of the reported magnetic phase transitions. The dependences of the QS and $\mu_0 H_{hf}$ values on Y concentration and on temperature are explained as mainly due to changes in the valence configuration of the Mn atoms. Good agreement is found between the orientation of the manganese magnetic moments in $LaMn_2Si_2$ as determined by the Mössbauer effect measurements and recent neutron diffraction measurements. The magnetic order above the previously reported ordering temperatures for the compounds with $x \leqslant 0.25$, indicated by the persisting magnetic hyperfine field (figure 4), is associated with an antiferromagnetic phase. Based on these Mössbauer effect results the magnetic phase diagram of the $La_{1-x}Y_xMn_2Si_2$ series was derived and found to be in good agreement with concurrent neutron diffraction findings [15, 24–26]. A spin-glass and/or frustrated magnetic system was found to exist within the critical region of these magnetic phase transitions.

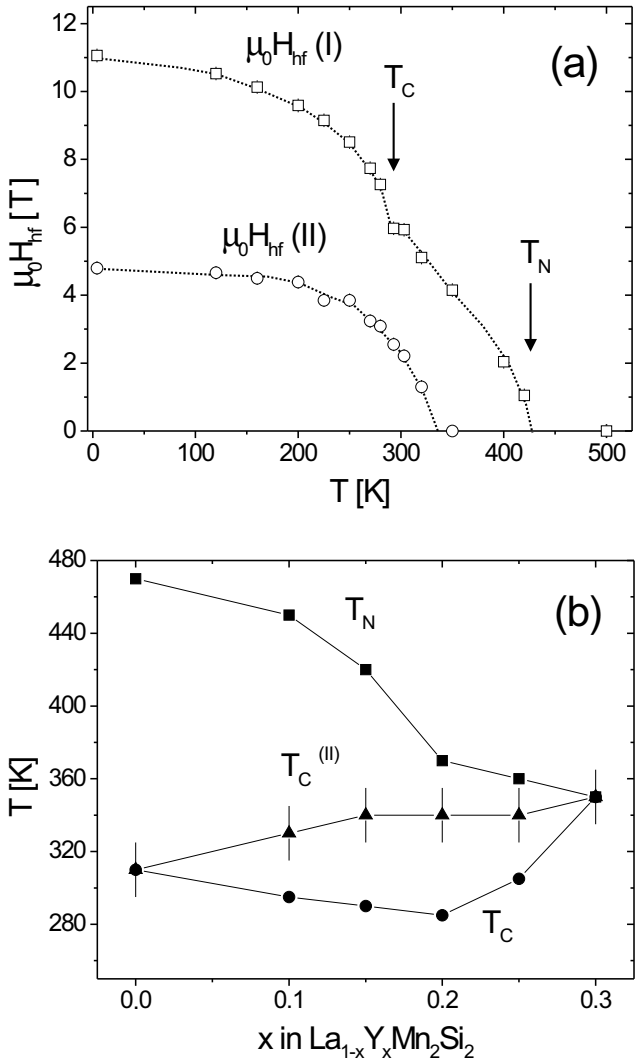

Figure 9. (a) Temperature dependences of the magnetic hyperfine field values of subspectra I and II, as derived from fits to the Mössbauer spectra of $La_{0.85}Y_{0.15}Mn_2Si_2$(^{57}Fe). The arrows indicate the Curie temperature T_C and the Néel temperature T_N (the dashed lines act as a guide to the eye). (b) Dependence of T_C^{II}, the temperature at which the hyperfine field of subspectrum II vanishes, as a function of yttrium concentration. The T_C and T_N values are also included for comparison.

Acknowledgments

This work was supported in part by grants from the Australian Research Council, leading to the award of a Research Scholarship and an ARC Research Fellowship. We also acknowledge access to the ISIS Facility, Rutherford Appleton Laboratory, UK (with support from the Access to Major Research Facilities Program; ANSTO, Lucas Heights Research Laboratories), and support from the Australian Institute of Nuclear Science and Engineering.

References

[1] Ban Z and Sikirika M 1965 *Acta Crystallogr.* **18** 594
[2] Szytula A and Leciejewicz J 1989 *Handbook on the Physics and Chemistry of Rare Earths* vol 12, ed K A Gschneidner Jr and L Eyring (Amsterdam: Elsevier) ch 83, pp 133–211
[3] Szytula A and Leciejewicz J 1994 *Handbook of Crystal Structures and Magnetic Properties of Rare Earth Intermetallics* (Boca Raton, FL: Chemical Rubber Company)
[4] Siek S, Szytula A and Leciejewicz J 1981 *Solid State Commun.* **39** 863
[5] Shigeoka T, Iwata N, Fujii H and Okamoto T 1985 *J. Magn. Magn. Mater.* **53** 83
[6] Szytula A and Siek S 1982 *J. Magn. Magn. Mater.* **27** 49
[7] Chaughule R S, Radhakrishnamurty C, Sampathkumaran E V, Malik S K and Vijayaraghavan R 1983 *Mater. Res. Bull.* **18** 817
[8] Sampathkumaran E V, Chaughule R S, Gopalakrishnan K V, Malik S K and Vijayaraghavan R 1983 *J. Less-Common Met.* **92** 35
[9] Fujii H, Inoda M, Okamoto T, Shigeoka T and Iwata N 1986 *J. Magn. Magn. Mater.* **54–57** 1345
[10] Kaneka T, Kanomata T, Yasui H, Shigeoka T, Iwata M and Nakagawa Y 1992 *J. Phys. Soc. Japan* **61** 4164
[11] Li Hong-Shuo, Cadogan J M, Zhao X L and Campbell S J 1994 *Hyperfine Interact.* **94** 1943
[12] Li Hong-Shuo, Cadogan J M, Zhao X L and Campbell S J 1995 *J. Magn. Magn. Mater.* **147** 91
[13] Hofmann M, Campbell S J, Zhao X L, Li Hong-Shuo and Cywinski R 1996 *Mater. Sci. Forum* **228–231** 587
[14] Venturini G, Welter R, Ressouche E and Malaman B 1994 *J. Alloys Compounds* **210** 213
[15] Hofmann M, Campbell S J, Kennedy S J and Zhao X L 1997 *J. Magn. Magn. Mater.* **176** 279
[16] Nowik I, Levi Y, Felner I and Bauminger E R 1995 *J. Magn. Magn. Mater.* **140–144** 913
[17] Nowik I, Levi Y, Felner I and Bauminger E R 1995 *J. Magn. Magn. Mater.* **147** 373
[18] Nowik I, Felner I and Bauminger E R 1996 *Nuovo Cimento* D **18** 275
[19] Nowik I, Felner I and Bauminger E R 1997 *Phys. Rev.* **55** 3033
[20] Nowik I, Levi Y, Felner I and Bauminger E R 1998 *J. Magn. Magn. Mater.* **185** 91
[21] Venturini G, Welter R, Ressouche E and Malaman B 1995 *J. Magn. Magn. Mater.* **150** 197
[22] Venturini G 1996 *J. Alloys Compounds* **232** 133
[23] Hofmann M, Campbell S J, Smith R, Kennedy S J, Zhao X L and Edge A V J 1998 *Mater. Sci. Forum* **278–281** 553
[24] Ijjaali I, Venturini G, Malaman B and Resouche E 1998 *J. Alloys Compounds* **266** 61
[25] Hofmann M, Campbell S J and Kennedy S J 1999 to be submitted
[26] Hofmann M, Campbell S J, Kennedy S J and Zhao X L 1999 in preparation
[27] Levin E M, Bodak O I, Gladyshevskii E I and Sinyushko V G 1992 *Phys. Status Solidi* a **134** 107
[28] Gütlich P 1975 *Mössbauer Spectroscopy (Topics in Applied Physics 5)* ed U Gonser (Berlin: Springer)
[29] Pauling L 1960 *The Nature of the Chemical Bond* (New York: Cornell University Press, Ithaca)
[30] Isoda S, Asano S and Ishida J 1986 *J. Phys. Soc. Japan* **55** 93
[31] Kulatov E, Veselago V and Vinokurova L 1990 *Acta Phys. Pol.* A **77** 709
[32] Welter R, Venturini G, Ressouche E and Malaman B 1995 *J. Alloys Compounds* **218** 204
[33] Williams A R, Morruzzi V L, Malozemoff A P and Terakura K 1983 *IEEE Trans. Magn.* **19** 1983
[34] Goodenough J B 1963 *Magnetism and The Chemical Bond* (New York: Wiley–Interscience)
[35] Li Hong-Shuo, Zhao X L, Campbell S J and Cadogan J M 1996 *Hyperfine Interact.* C **1** 123